

## TECHNICAL REPORT

# Application of fused image in detecting abnormalities of temporomandibular joint

<sup>1</sup>Ruo-Han Ma, <sup>1</sup>Gang Li, <sup>2</sup>Yi Sun, <sup>3,4</sup>Juan-Hong Meng, <sup>1,4</sup>Yan-Ping Zhao and <sup>4,5</sup>Hao Zhang

<sup>1</sup>Department of Oral and Maxillofacial Radiology, Peking University School and Hospital of Stomatology, Beijing, China;

<sup>2</sup>Department of Imaging & Pathology, University of Leuven and Oral & Maxillofacial Surgery, University Hospitals Leuven,

Leuven, Belgium; <sup>3</sup>Department of Oral and Maxillofacial Surgery, Peking University School and Hospital of Stomatology, Beijing, China; <sup>4</sup>Center for Temporomandibular Disorders and Orofacial Pain, Peking University School and Hospital of Stomatology,

Beijing, China; <sup>5</sup>Department of Prosthodontics, Peking University School and Hospital of Stomatology, Beijing, China

**Objectives:** To present a method for image fusion of cone beam CT (CBCT)/CT and MRI and to explore whether the image data sets fused in such a way could aid the detection of temporomandibular joint (TMJ) anatomical structures and lesions.

**Methods:** There were five cases included in this study. One case was space occupying lesion giant cell tumour of tendon sheaths, one case was chronic inflammation in the condyle, one case was articular disc calcification of the bilateral TMJs, and the other two cases were TMJ disorders (anterior disc displacement without reduction). The digital imaging and communications in medicine format data of CT/CBCT and MRI of the cases were collected, and then imported to the Amira visual software where the registration process was conducted. Based on the different scan model, the registration process could be separated into automatic registration of CT/CBCT with quadrature slice MR images and the semi-automatic registration of CT/CBCT with oblique slice MR images by altering the registration parameters. Rigid transform model and the similarity metric of normalization mutual information was used for registration in the present study.

**Results:** The relationship between the soft mass and hard tissue was shown clearly in the fused images when compared to sole observation of CBCT/CT or MR images. The fused images could define the tumour outline and the destructive bone clearly in the same image. The fused results helped the observers to ensure uncertain defects which could not be confirmed only by one image data set.

**Conclusions:** The CT/CBCT and MR images could be fused to aid detection of TMJ anatomical structures and related lesions.

*Dentomaxillofacial Radiology* (2019) **48**, 20180129. doi: [10.1259/dmfr.20180129](https://doi.org/10.1259/dmfr.20180129)

**Cite this article as:** Ma R-H, Li G, Sun Y, Meng J-H, Zhao Y-P, Zhang H. Application of fused image in detecting abnormalities of temporomandibular joint. *Dentomaxillofac Radiol* 2019; **48**: 20180129.

**Keywords:** temporomandibular joint; diagnosis; cone-beam computed tomography; multi-detector computed tomography; magnetic resonance imaging

## Introduction

Temporomandibular joint (TMJ) is one of the most complex joint in human anatomic structures. TMJ diseases include several categories, such as temporomandibular joint disorders (TMD), ankylosis, trauma,

TMJ cyst or tumours. For detecting the TMJ diseases, many diagnostic imaging techniques have been proposed, such as panoramic radiography, axially corrected sagittal tomography, ultrasonography, MRI, CT and cone beam CT (CBCT). Plain films present limitations due to the superimposition of surrounding structures around the region of interest. Previous

Correspondence to: Dr Gang Li, E-mail: [kqgang@bjmu.edu.cn](mailto:kqgang@bjmu.edu.cn)

Received 01 April 2018; revised 22 November 2018; accepted 27 November 2018

studies demonstrate that the display of osteophytes in panoramic image is poor,<sup>1,2</sup> and only extensive erosions and large osteophytes in the TMJ can be identified.<sup>3</sup> Although ultrasonography is reliable in assessing condylar erosions, it has limitations to the anterior and lateral aspects of the TMJ.<sup>4</sup>

In consideration of the anatomic structures of TMJ and the imaging shortcomings of the above-mentioned modalities, CT/CBCT and MRI have obvious advantages in assessing TMJ-related lesions. Researches have demonstrated that CT is a suitable method for examining bone changes of TMJ.<sup>3</sup> Also, the superiority of CT in displaying the features of TMJ osteoarthritis has been well-documented and widely accepted.<sup>5</sup> Westesson *et al*<sup>6</sup> states that CT had higher diagnostic accuracy and depicted the osseous abnormalities with finer details than MRI. However, relatively high radiation dose limits its use in oral and maxillofacial examinations. Compared with CT, CBCT has the advantages of providing high resolution images at a low radiation dose level.<sup>7-9</sup> Several studies<sup>6-10</sup> have shown that the diagnostic capabilities of CBCT is equal to or greater than those of CT. CBCT is a diagnostic alternative for detecting bone defects in the TMJ with consideration of financial and irradiation reasons.<sup>10-12</sup> Because of the low contrast resolution of CBCT, CT could not be replaced in detecting soft tissue tumours or tumour-like lesions. In terms of detecting soft tissues of TMJ, MRI is an alternative method. MRI not only provides morphological information of TMJ area with high resolution but also reflects the status of effusion and the changes of bone marrow.<sup>13-15</sup> MRI has already been considered as a method of choice for evaluation of the amount of joint fluid.<sup>16</sup>

Apparently, due to the different limitations, none of the above-mentioned imaging methods could provide sufficient information for TMJ region, which includes temporomandibular fossa, condyle, surrounding soft tissues and the possible joint fluid. Hence, a method with more accurate and reliable identification of TMJ and related lesions is desired. In 1990s, a technique called image fusion was introduced. This technique can be used to merge characteristics of images from different modalities so that certain features can be enhanced, which is not visible in either of the single data alone. Besides, the missing information in one image can be substituted with signals from another sensor image after the process of image fusion. Gedrange *et al*<sup>17</sup> compared the measurement and visualization of the TMJ by using CT and MRI independently, and indicated that maximum information could be obtained using both imaging techniques together due to the synergistic effects. This indicates that the recognition of TMJ structures may be improved from the CT and MRI-fused data set images. Thus, the aim of the present study was to present a method for image fusion and to explore whether the image data sets fused in such a way could aid the detection of TMJ anatomical structures and lesions in five clinical cases.

## Methods and materials

### Subjects

Five patients were collected from the Center for Temporomandibular Disorders and Orofacial Pain in Peking University School and Hospital of Stomatology for the first visits from 2010 to 2017. For diagnostic purpose, all the five patients were captured with MRI and CT/CBCT scans. The details of scanning parameters for each case were shown in Table 1. All the image data were exported as digital imaging and communications in medicine format.

All the subject recruitment were approved by the Ethics Committee of Peking University School and Hospital of Stomatology (PKUSSIRB-201520035). Informed consent was obtained from all subjects (participants or their legal guardians) for publication of the present study, including accompanying images. All methods were carried out in accordance with relevant guidelines and regulations.

### Imaging registration and fusion

The DICOM format data of CT/CBCT and MRI were imported to the Amira visual software (v. 5.4.3, Visage Imaging, Melbourne, Australia), and the registered process was conducted in the subapplication of the multiplanar viewer module.

Amira software is not specialized in registration and fusion of images. In the present study, the process of multimodality images automatic/semi-automatic registration, which aimed to the fusion of TMJ images, had been achieved by adjusting the registration parameters. It was important to note that there was no marker on the patients' skin surface at the time of scanning and all of the registration process were conducted without any help of markers.

There were two kinds of MRI scan methods for the collected cases. One is the sagittal and coronal views of patients' head, which were acquired by the quadrature head coil. This scan model is for the patients suffered from tumours or tumour-like lesions. The other is the oblique sagittal and oblique coronal views of two TMJs, which were obtained by the 3-inch surface coils. This scan method is usually for the patients with TMD or diseases limited in TMJ structures. The two scanning protocols would determine whether the registration process is a full-automatically procedure, or not. Therefore, based on the different scan model, the registration process could be separated into two types, one is automatic registration of CT/CBCT with quadrature slice MR images, and the other is semi-automatic registration of CT/CBCT with oblique slice MR images by altering the registration parameters.

In the present study, the CT/CBCT images were fixed while the MR images were mobile when the registration was conducted. In other words, the MRI layers were on the top of CT/CBCT layers while registering. In order to facilitate observation, all of the bone image layers

**Table 1** The details of scanning parameters for each case

	CT	CBCT	MRI
Case 1	GE BrightSpeed <sup>a</sup> 140 kV, 39 mAs slice thickness 2.5 mm supine position	N/A	SIEMENS Novus (1.5T) <sup>c</sup> Axial/sag/cor <sup>d</sup> position T1 (TR: 410 ms; TE: 10 ms), T2 (TR: 5300 ms; TE: 100 ms) voxel size: 0.5273 × 0.5273 mm slice thickness: 5 mm
Case 2	N/A	3DX CBCT <sup>b</sup> 80 kV, 45 mAs FOV: 4 × 4 cm voxel size: 0.125 × 0.125 mm	SIEMENS Sonata (1.5T) axial/osag/ocor position T1 (TR: 350 ms; TE: 15 ms), T2 (TR: 2790 ms; TE: 103 ms); PD (TR: 2790 ms; TE: 13 ms) voxel size: 0.3125 × 0.3125 mm Slice thickness: 4/3 mm(for axial)
Case 3	N/A	3D Accuitomo 170 CBCT 90 kV, 45 mAs FOV: 6 × 6 cm voxel size: 0.125 × 0.125 mm.	SIEMENS Trio Tim (3.0 T) axial/osag/ocor position T1 (TR: 250 ms; TE: 2.7 ms), T2 (TR: 4120 ms; TE: 99 ms); PD (TR: 4120 ms; TE: 20 ms) voxel size: 0.2344 × 0.2344 mm/0.5469 × 0.5469 mm Slice thickness: 3 mm
Case 4	N/A	3D Accuitomo 170 CBCT 90 kV, 45 mAs FOV: 6 × 6 cm voxel size: 0.125 × 0.125 mm.	GE OPTIMA MR360 (1.5T) axial/osag/ocor position T1 (TR: 338–494 ms; TE: 10–11 ms), T2 (TR: 2000 ms; TE: 106 ms); PD fs (TR: 1993 ms; TE: 32 ms); PD (TR: 1771 ms; TE: 47 ms) voxel size: 0.3906 × 0.3906 mm Slice thickness: 2.5/3 mm (for axial)
Case 5	N/A	3D Accuitomo 170 CBCT 90 kV, 45 mAs FOV: 6 × 6 cm voxel size: 0.125 × 0.125 mm.	GE Medical system Signa HDxt (1.5T) axial/osag/ocor position T1 (TR: 733 ms; TE: 10 ms), T2 (TR: 4383 ms; TE: 102 ms); T2 fs(TR: 3350 ms; TE: 84 ms); PD (TR: 1950 ms; TE: 22 ms) voxel size: 0.2344 × 0.2344 mm Slice thickness: 2/2.6 mm (for osag)

CBCT, cone beam CT; FOV, field of view; PD, proton density; TE, echo time; TR, repetition time.

<sup>a</sup>CT: GE Medical system BrightSpeed CT scanner (General Electric Company, Connecticut, CT);

<sup>b</sup>CBCT: 3DX, 3D Accuitomo 170 (J. Morita MFG, Corp., Irvine, CA);

<sup>c</sup>MRI: SIEMENS Novus, SIEMENS Sonata, SIEMENS Trio Tim (Siemens AG, Munich, Germany); GE Medical system OPTIMA MR360, GE Medical system Signa HDxt (General Electric Company, Connecticut, CT);

<sup>d</sup>sag: sagittal; cor: coronal; osag: oblique sagittal; ocor: oblique coronal; fs: fat suppression.

(CT/CBCT) were in yellow colour gradation while the soft tissue layers in greyscale (MR images). The similarity metric of all CT/CBCT and MR images registration was normalization mutual information, which could solve the problem that the mutual information is sensitive to the decrease of two image overlapped areas<sup>18</sup> besides rigid transform model was used for both kinds of registration. For automatic registration, two image sets should be first aligned in centre, which was an automatic process, and then the registration would proceed automatically. Other parameters just maintained the default values and there were no need to vary any other conditions. While for semi-automatic registration, *i.e.* registration of CT/CBCT and oblique slice MR images, the operators need to adjust two image sets to aligned position roughly by using the manual registration tool. Subsequently, the Conjugated Gradients was chosen as the optimizer. The finest level was 0 for Gradient optimizer and the tolerance was 0.0001. The setting of coarsest resampling was adjusted to  $x = 2$ ,  $y = 2$  and  $z = 2$ . The histogram range reference was from -200 to 2500 and the histogram range model was from 150 to 1400. The reference of histogram bins was 245 and the model was 250. With these parameter design, the registration process was faster and more precise and repeatable in registering. Meanwhile, less user interaction could decrease the operation time effectively. The time required for the manual registration was about 3–5 min. The automatic process could be completed within 40 s.

## Results

Within the five cases presented in the present study, one case was space occupying lesion giant cell tumour of tendon sheaths (GCTTS), one case was chronic inflammation in the condyle and one case was articular disc calcification of the bilateral TMJs. The other two cases were TMD (anterior disc displacement without reduction). The relationships between normal and abnormal structures were shown clearly in the fused images when compared to sole observation of CBCT/CT or MR images.

### Case one: Fused images from CT and MRI for GCTTS of TMJ (Figure 1)

A 45-year-old female had suffered from uncomfatableness in the maxillofacial region for 2 years. The CT bone window images (Figure 1a) showed that the left skull base was partially invaded. From the soft tissue window images (Figure 1b), there was a mass with fairly clear demarcation in the left TMJ region, and the internal density was not uniform. From the MR images (Figure 1c,d), especially in  $T_2$  weighted imaging ( $T_2$ WI, Figure 1d), a well-demarcated low signal intensity mass was shown in the left TMJ area and the tumour involved masseter, infratemporo- and temporo space. The low signal inside the tumour could be seen in both  $T_1$  weighted imaging ( $T_1$ WI) and  $T_2$ WI, which

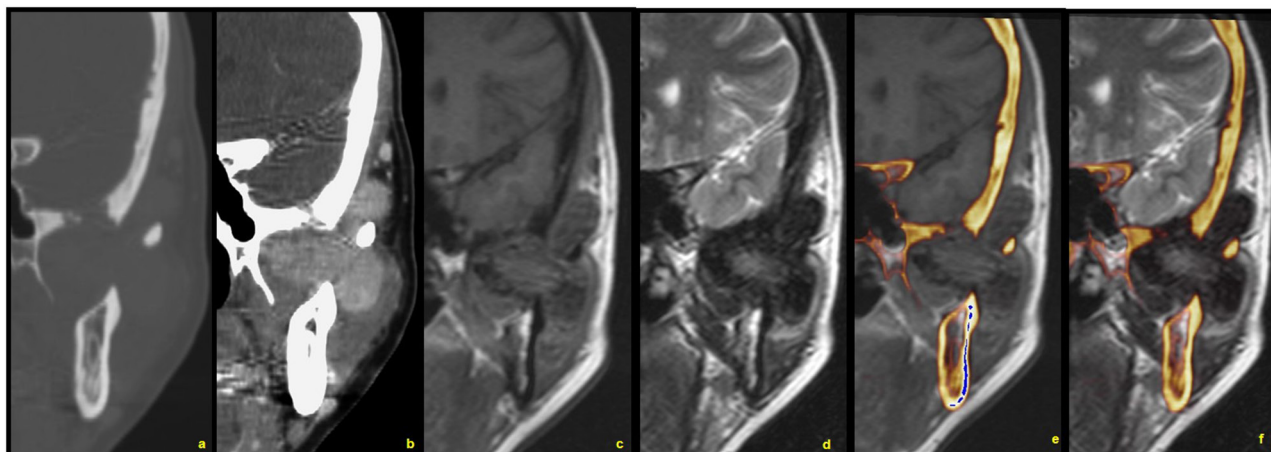


**Figure 1** Fusion images coronal view for case one. (a: CT images in bone window; b: CT images in soft tissue window; c: MR images in  $T_1$ WI; d: MR images in  $T_2$ WI; e: CT-MR ( $T_1$ ) fused images; f: CT-MR ( $T_2$ ) fused images).  $T_1$ WI,  $T_1$  weighted imaging;  $T_2$ WI,  $T_2$  weighted imaging.

is an MRI non-specific distinctive manifestations of tendon sheaths giant cell tumour. However, all the hard tissues were confused with the soft tissue lesion in the MR images, and most of clinicians could not determine the bone defects which were caused by the soft mass just through the MR images. **Figure 1e and f** are the fused images from **Figure 1a,c,d** respectively. The fused images show the bone defects and the soft tissue lesion simultaneously. The pathological diagnosis of this case was identified as GCTTS.

*Case two: Fused images from CBCT and MRI for chronic inflammation of the condyle (Figure 2)*

A 31-year-old male had been suffered from open-mouth limitation with pain of the right TMJ region for a month. From the CBCT images, the decreased density of the right condyle could be observed, and most of the cortical and the trabecular bone were destroyed (**Figure 2a,d**). The MR images showed the mixed-signal mass with ill-defined margins in  $T_1$ WI and  $T_2$ WI (**Figure 2b,e**). However, the hard-tissue was difficult to be observed in the MR images. The fused images of CBCT and MRI could overcome the weaknesses of both CBCT and MR images (**Figure 2c,f**). The pathological diagnosis of this case was chronic inflammation of the right condyle.

*Case three: Fused images from CBCT and MRI for articular disc calcification of the bilateral TMJs (Figure 3)*

A 61-year-old female had suffered from pain with click in the left TMJ and masseter region for a month. From the CBCT images, a rod-like high-density could be observed in each of the TMJ space. The high densities looked like a calcification of TMJ disks, however, merely by CBCT images this relationship could not be defined (**Figure 3a,d**). Thus, an MR examination was undertaken. There were no obvious abnormality in proton density weighted imaging and T2WI MR images

(**Figure 3b,e**). With these images, the clinicians could not confirm whether the calcification related to the disc or not. However, the fused images of CBCT and MRI could answer the question definitely. From the fused images, one could definitely observe that the high-densities were just located in the bilateral discs (**Figure 3c,f**). Thus, the source and the nature of the calcifications

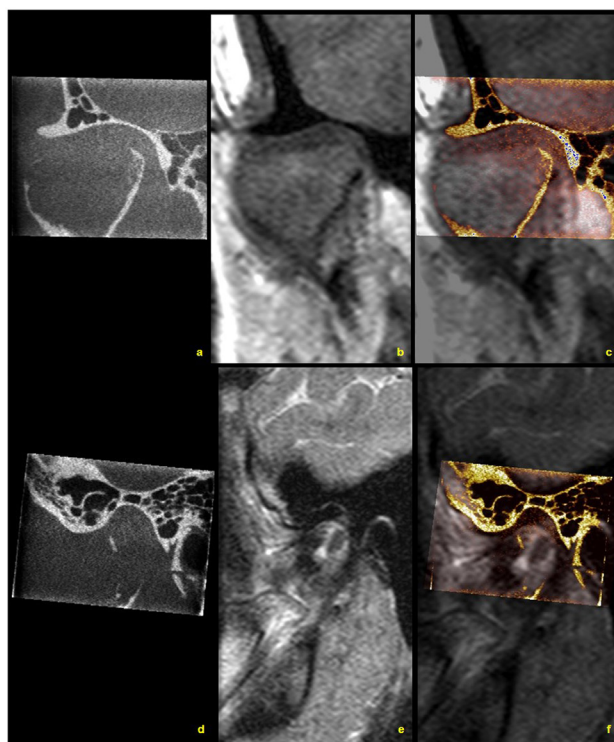


**Figure 2** Fusion images for case two. (a-c are in coronal view; d-f are in sagittal view; a, d: CBCT images; b: MR images in  $T_1$ WI; e: MR images in  $T_2$ WI; c, f: CT-MR ( $T_1/T_2$ ) fused images). CBCT, cone beam CT;  $T_1$ WI,  $T_1$  weighted imaging;  $T_2$ WI,  $T_2$  weighted imaging.

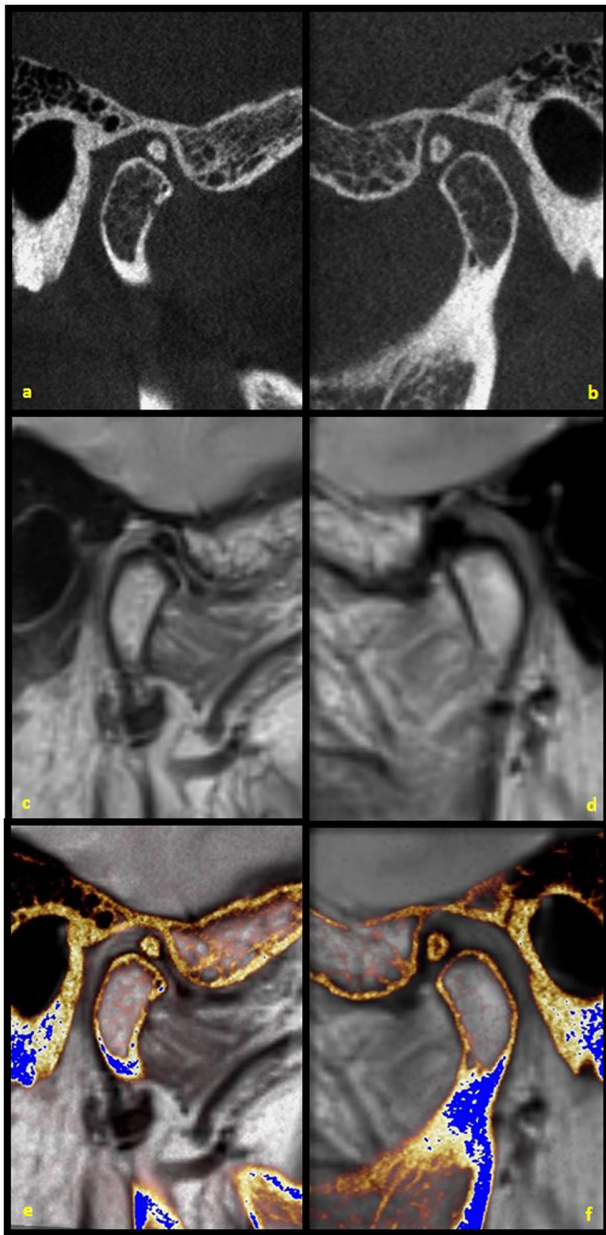


**Figure 3** Fusion images for case three. (a, c, e are left TMJ images in oblique sagittal view; b, d, f are right TMJ images in oblique sagittal view; a, b are CBCT images; c, d are MR images in PDWI; e, f are CBCT-MR (PD) fusion images). CBCT, cone beam CT; PDWI, proton density weighted imaging; TMJ, temporo mandibular joint.

could be clearly discovered by the method of image fusion.

*Fused images from CBCT and MRI for TMD*

**Case four: Anterior disc displacement without reduction (Figure 4):** A 52-year-old female presented with the complaint of right TMJ region pain and open-mouth limitation for the latest 3 months. From the CBCT images (Figure 4a,d), the cortical bone of the mandibular

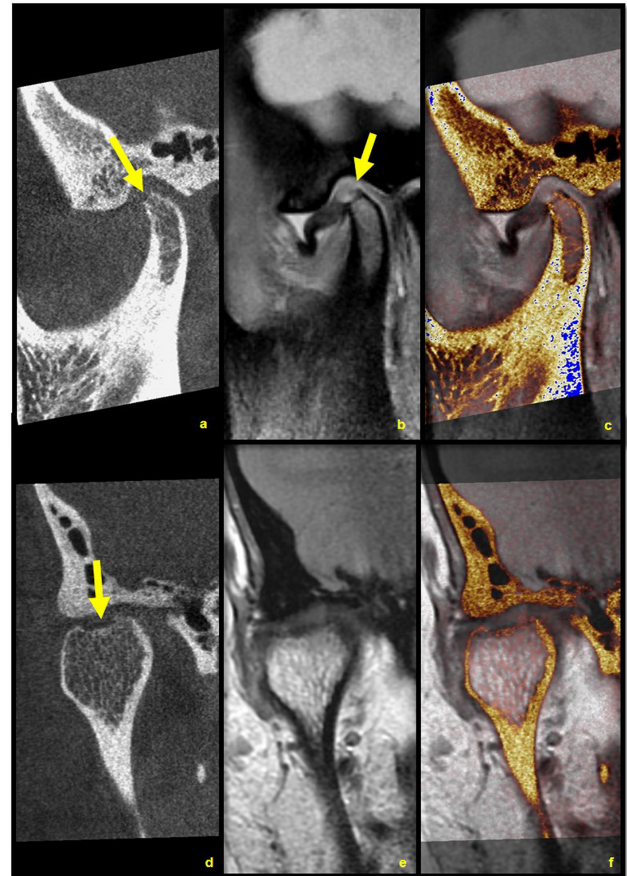


**Figure 4** Fusion images for Case 4. (a–c are in oblique sagittal view; d–f are in oblique coronal view; a, d: CBCT images; b, e: MR images in PDWI; c, f: CBCT-MR (PD) fusion images). CBCT, cone beam CT; PDWI, proton density weighted imaging.

condyle was almost intact in sagittal and coronal views, but a concave shape could be seen in coronal views (the yellow arrows in Figure 4a,d). The radiologists were unsure that if it was a primary deformity or deformed by compression of soft tissue swelling. From the images in Figure 4b and e, which were proton density weighted imaging of MR images, the anterior disk displacement and the effusion were shown clearly. Besides, the swelling of the disk posterior attachment was also presented and the cortical bone was involved in sagittal and coronal views (the yellow arrow in Figure 4b). However, the exact bone changes was not definite especially in coronal view. In the fused images in Figure 4c and f, the observers could ensure that the disk was anteriorly displaced, the swelling attachment compressed the condyle to concave deformity but the cortical bone was still intact. The final clinical diagnosis of this patient was anterior disc displacement without reduction.

**Case five: Anterior disc displacement without reduction (Figure 5)**

A 14-year-old female presented with the complaint of pain in the left TMJ and open-mouth limitation for

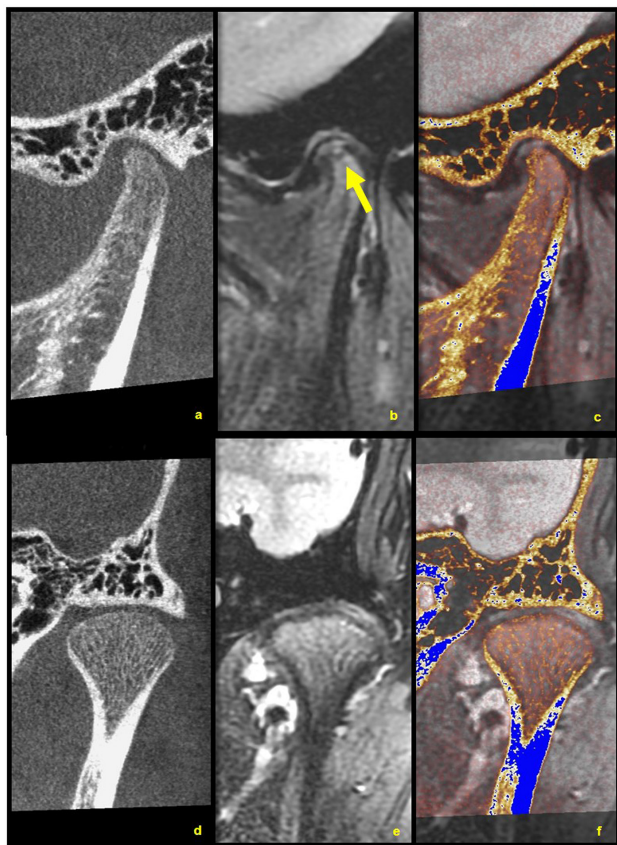


**Figure 5** Fusion images for Case 5. [a–c are in oblique sagittal view; d–f are in oblique coronal view; a, d: CBCT images; b, e: MR images in  $T_2$ WI; c, f: CBCT-MR ( $T_2$ ) fused images]. CBCT, cone beam CT.

about 2 days. The patient had the history of clicking in the left TMJ during mouth opening. From the  $T_2$ WI MR images (Figure 5b,e), the disk was anteriorly displaced and there was a doubtful defects on the top of condyle in the sagittal views (the yellow arrow in Figure 5b) in spite of the cortical and cancellous bone was in a good condition in the coronal views. Meanwhile, from the CBCT images (Figure 5a,d), the morphology of the condyle was normal and there was no obvious cortical bone on the top of the condyle because of the young age of the patient. The fused images (Figure 5c and f), however, showed the soft and bone tissue conditions at the same time. From the fused images, the investigators could ensure not only the anterior disk displacement of the patient, but also the normal substance of bone which was a suspected bone defect in the MR images. The clinical diagnosis of this patient was anterior disc displacement without reduction.

## Discussion

Image fusion has been investigated and used in clinic of oral and maxillofacial region for decades,<sup>19</sup> and several methods for image fusion from multiimaging

modalities have been introduced.<sup>20–22</sup> However, only a few reports were published and the usefulness of the fused image for the observation of TMJ still needs further investigation.

Based on the fact that few imaging methods could capture a complete structure information, image fusion could be an alternative for this difficulty. For detecting the TMJ diseases, the reliability and accuracy of image interpretation may be improved by complementing each image's advantages.

For Case 1, the internal signal of GCTTS and the circumstances of the soft tissue and synovium were well shown in the MR images, but not the extent of the osseous destruction. Meanwhile, the osseous destruction was clearly depicted in the bone window of CT images. When the two image data sets were fused, the relationship between the soft mass and the hard tissue was clearly observed when compared to sole observation of CT or MR images. From the second case, the destroyed bone was showed exactly in the fused images when compared to the MR images. Not only were the conditions of the bone and soft tissues but also the nature of the disease even demonstrated in the fused images. In the third case, the calcified disc could not be defined in either of CBCT and MR images. However, the fused images clearly indicated that the calcification was within the disc.

Al-saleh et al<sup>23</sup> compared the interobserver consistency between the students and experienced radiologists in MRI and MRI–CBCT fusion images to determine the position of the articular disc. The results showed that the interobserver consistency was very low when observing the MRI alone, while the consistency was relatively high when using MRI–CBCT fused image. Similarly, a previous study by comparing MRI and MRI–CBCT fused images demonstrated that the intra- and interobserver agreement for detecting the disk position could be improved significantly in MRI–CBCT fused image.<sup>24</sup> In our study, for the cases with TMD, the conditions of the soft and bony tissue could be determined and the position of the disc could be identified by observing the fused images of CBCT and MRI. In addition, it may be difficult to definitely read and identify MR images or some parts of CT images for junior dentists, junior oral and maxillofacial surgeons or radiologists. The fusion of images from different imaging modalities could make TMJ anatomic structures displayed visibly. This would be beneficial to the junior clinicians who do not have much experiences in reading radiographs, especially in reading MR and CT images.<sup>25</sup> This is also beneficial to the work of clinical education and practice.

In this report, there are two kinds of MRI scan methods employed and subsequently produce two kind of MR images, *i.e.* quadrature slice MRI and oblique slice MRI. Since the initialized position used to take MR images with these two modes are different, the images has to be adjusted in the pre-registration

process. For the sagittal and coronal views of MRI images, the initialized positions of MRI and CBCT images are similar, so the process of pre-registration is automatic. However, with the oblique sagittal and oblique coronal views of MRI images, the initialized positions of MRI and CBCT images are totally different, so it needs to conduct the image pre-registration process manually.

The multimodality image fusion may be considered as a technique of choice when there is a need to investigate the bony and the soft tissue changes simultaneously. Technically, however, the process of registration and fusion of multimodality images would cause the qualitative loss of the raw images. Hence, the technical disadvantage may lead to the limitation of finding tiny defects when compared to observation of one image data sets. This may

be the concern of majority of clinicians, and this disadvantage may challenge the future investigation.

### Acknowledgment

The authors deny any conflicts of interest related to this study.

### Funding

The study was supported by Beijing Municipal Science & Technology Commission (No. 151100004015040) and National Natural Science Foundation of China (No. 81671034).

### References

1. Masood F, Katz JO, Hardman PK, Glaros AG, Spencer P. Comparison of panoramic radiography and panoramic digital subtraction radiography in the detection of simulated osteophytic lesions of the mandibular condyle. *Oral Surg Oral Med Oral Pathol Oral Radiol Endod* 2002; **93**: 626–31.
2. Ludlow JB, Davies KL, Tyndall DA. Temporomandibular joint imaging: a comparative study of diagnostic accuracy for the detection of bone change with biplanar multidirectional tomography and panoramic images. *Oral Surg Oral Med Oral Pathol Oral Radiol Endod* 1995; **80**: 735–43.
3. Hussain AM, Packota G, Major PW, Flores-Mir C. Role of different imaging modalities in assessment of temporomandibular joint erosions and osteophytes: a systematic review. *Dentomaxillofac Radiol* 2008; **37**: 63–71. doi: <https://doi.org/10.1259/dmfr/15831361>
4. Rudisch A, Emshoff R, Maurer H, Kovacs P, Bodner G. Pathologic-sonographic correlation in temporomandibular joint pathology. *Eur Radiol* 2006; **16**: 1750–6. doi: <https://doi.org/10.1007/s00330-006-0162-0>
5. Ahmad M, Hollender L, Anderson Q, Kartha K, Ohrbach R, Truelove EL, et al. Research diagnostic criteria for temporomandibular disorders (RDC/TMD): development of image analysis criteria and examiner reliability for image analysis. *Oral Surg Oral Med Oral Pathol Oral Radiol Endod* 2009; **107**: 844–60. doi: <https://doi.org/10.1016/j.tripleo.2009.02.023>
6. Westesson PL, Katzberg RW, Tallents RH, Sanchez-Woodworth RE, Svensson SA. CT and MR of the temporomandibular joint: comparison with autopsy specimens. *AJR Am J Roentgenol* 1987; **148**: 1165–71. doi: <https://doi.org/10.2214/ajr.148.6.1165>
7. De Vos W, Casselman J, Swennen GR. Cone-beam computerized tomography (CBCT) imaging of the oral and maxillofacial region: a systematic review of the literature. *Int J Oral Maxillofac Surg* 2009; **38**: 609–25. doi: <https://doi.org/10.1016/j.ijom.2009.02.028>
8. Qu XM, Li G, Zhang ZY, Ma XC. Comparative dosimetry of dental cone-beam computed tomography and multi-slice computed tomography for oral and maxillofacial radiology. *Zhonghua Kou Qiang Yi Xue Za Zhi* 2011; **46**: 595–9.
9. Ludlow JB, Ivanovic M. Comparative dosimetry of dental CBCT devices and 64-slice CT for oral and maxillofacial radiology. *Oral Surg Oral Med Oral Pathol Oral Radiol Endod* 2008; **106**: 106–14. doi: <https://doi.org/10.1016/j.tripleo.2008.03.018>
10. Zain-Alabdeen EH, Alsadhan RI. A comparative study of accuracy of detection of surface osseous changes in the temporomandibular joint using multidetector CT and cone beam CT. *Dentomaxillofac Radiol* 2012; **41**: 185–91. doi: <https://doi.org/10.1259/dmfr/24985971>
11. Honda K, Larheim TA, Maruhashi K, Matsumoto K, Iwai K. Osseous abnormalities of the mandibular condyle: diagnostic reliability of cone beam computed tomography compared with helical computed tomography based on an autopsy material. *Dentomaxillofac Radiol* 2006; **35**: 152–7. doi: <https://doi.org/10.1259/dmfr/15831361>
12. Hussain AM, Packota G, Major PW, Flores-Mir C. Role of different imaging modalities in assessment of temporomandibular joint erosions and osteophytes: a systematic review. *Dentomaxillofac Radiol* 2008; **37**: 63–71. doi: <https://doi.org/10.1259/dmfr/16932758>
13. Tomura N, Otani T, Narita K, Sakuma I, Takahashi S, Watarai J, et al. Visualization of anterior disc displacement in temporomandibular disorders on contrast-enhanced magnetic resonance imaging: comparison with T2-weighted, proton density-weighted, and precontrast T1-weighted imaging. *Oral Surg Oral Med Oral Pathol Oral Radiol Endod* 2007; **103**: 260–6. doi: <https://doi.org/10.1016/j.tripleo.2006.02.003>
14. Tasaki MM, Westesson PL. Temporomandibular joint: diagnostic accuracy with sagittal and coronal MR imaging. *Radiology* 1993; **186**: 723–9. doi: <https://doi.org/10.1148/radiology.186.3.8430181>
15. Emshoff R, Gerhard S, Ennemoser T, Rudisch A. Magnetic resonance imaging findings of internal derangement, osteoarthritis, effusion, and bone marrow edema before and after performance of arthrocentesis and hydraulic distension of the temporomandibular joint. *Oral Surg Oral Med Oral Pathol Oral Radiol Endod* 2006; **101**: 784–90. doi: <https://doi.org/10.1016/j.tripleo.2005.09.005>
16. Gil C, Santos KC, Dutra ME, Kodaira SK, Oliveira JX. MRI analysis of the relationship between bone changes in the temporomandibular joint and articular disc position in symptomatic patients. *Dentomaxillofac Radiol* 2012; **41**: 367–72. doi: <https://doi.org/10.1259/dmfr/79317853>
17. Gedrange T, Gredes T, Hietschold V, Kunert-Keil C, Dominiak M, Gerber H, et al. Comparison of reference points in different methods of temporomandibular joint imaging. *Adv Med Sci* 2012; **57**: 157–62. doi: <https://doi.org/10.2478/v10039-012-0007-9>
18. XF L, Zhang CL, HP L, Zang XB. Development of medical image registration technology (in Chinese). *Computer Science* 2010; **7**: 27–33.
19. Plooi JM, Maal TJ, Haers P, Borstlap WA, Kuijpers-Jagtman AM, Bergé SJ. Digital three-dimensional image fusion processes for planning and evaluating orthodontics and orthognathic surgery. A systematic review. *Int J Oral Maxillofac Surg* 2011; **40**: 341–52. doi: <https://doi.org/10.1016/j.ijom.2010.10.013>

20. Zandieh S, Bernt R, Mirzaei S, Haller J, Hergan K. Image fusion between 18F-FDG PET and MRI in cardiac sarcoidosis: A case series. *J Nucl Cardiol* 2018; **25**: 1128–34. doi: <https://doi.org/10.1007/s12350-016-0653-6>
21. Fenstermaker M, Mendhiratta N, Bjurlin MA, Meng X, Rosenkrantz AB, Huang R, et al. Risk stratification by urinary prostate cancer gene 3 testing before magnetic resonance imaging-ultrasound fusion-targeted prostate biopsy among men with no history of biopsy. *Urology* 2017; **99**: 174–9. doi: <https://doi.org/10.1016/j.urology.2016.08.022>
22. Lai WJ, Wang HK, Liu HT, Park BK, Shen SH, Lin TP, et al. Cognitive MRI-TRUS fusion-targeted prostate biopsy according to PI-RADS classification in patients with prior negative systematic biopsy results. *J Chin Med Assoc* 2016; **79**: 618–24. doi: <https://doi.org/10.1016/j.jcma.2016.05.004>
23. Al-Saleh MAQ, Alsufyani N, Lai H, Lagravere M, Jaremko JL, Major PW. Usefulness of MRI-CBCT image registration in the evaluation of temporomandibular joint internal derangement by novice examiners. *Oral Surg Oral Med Oral Pathol Oral Radiol* 2017; **123**: 249–56. doi: <https://doi.org/10.1016/j.oooo.2016.10.016>
24. Al-Saleh MA, Alsufyani NA, Lagravere M, Nebbe B, Lai H, Jaremko JL, et al. MRI alone versus MRI-CBCT registered images to evaluate temporomandibular joint internal derangement. *Oral Surg Oral Med Oral Pathol Oral Radiol* 2016; **122**: 638–45. doi: <https://doi.org/10.1016/j.oooo.2016.07.024>
25. Dai J, Dong Y, Shen SG. Merging the computed tomography and magnetic resonance imaging images for the visualization of temporomandibular joint disk. *J Craniofac Surg* 2012; **23**: e647–e648. doi: <https://doi.org/10.1097/SCS.0b013e3182710517>